

## Supporting Information

### Photophysics and Electrochemistry of a Platinum-Acetylide Disubstituted Perylene-3,4,9,10-tetracarboxylic diimide

Ben A. Llewellyn,<sup>a</sup> Anna G. Slater,<sup>a</sup> Gudrun Goretzki,<sup>a</sup> Timothy L. Easun,<sup>a</sup> E. Stephen Davies,<sup>a</sup> Stephen P. Argent,<sup>a</sup> William Lewis,<sup>a</sup> Andrew Beeby,<sup>b</sup> Michael W. George<sup>a</sup> and Neil R. Champness<sup>a\*</sup>

#### Electrochemistry Measurements.

Compound	1 <sup>st</sup> reduction	2 <sup>nd</sup> reduction	Oxidation	$\Delta E(\text{Fc}^+/\text{Fc})$
<b>1</b>	-1.22 (0.10)	-1.46 (0.09)	+0.71 <sup>#</sup>	(0.08)
<b>2</b>	-1.21 (0.08)	-1.44 (0.07)	+0.72 <sup>#</sup>	(0.08)

Potentials reported as  $E_{1/2}$  ( $= (E_p^a + E_p^c)/2$ ) in V vs.  $\text{Fc}^+/\text{Fc}$  at  $0.1 \text{ Vs}^{-1}$  scan rate and quoted to the nearest 0.01 V. Values in parentheses are  $\Delta E$  ( $= E_p^a - E_p^c$ ) for the couple at  $0.01 \text{ Vs}^{-1}$ . <sup>#</sup> Peak maximum from square wave voltammetry

#### EPR Measurements for reduced species.

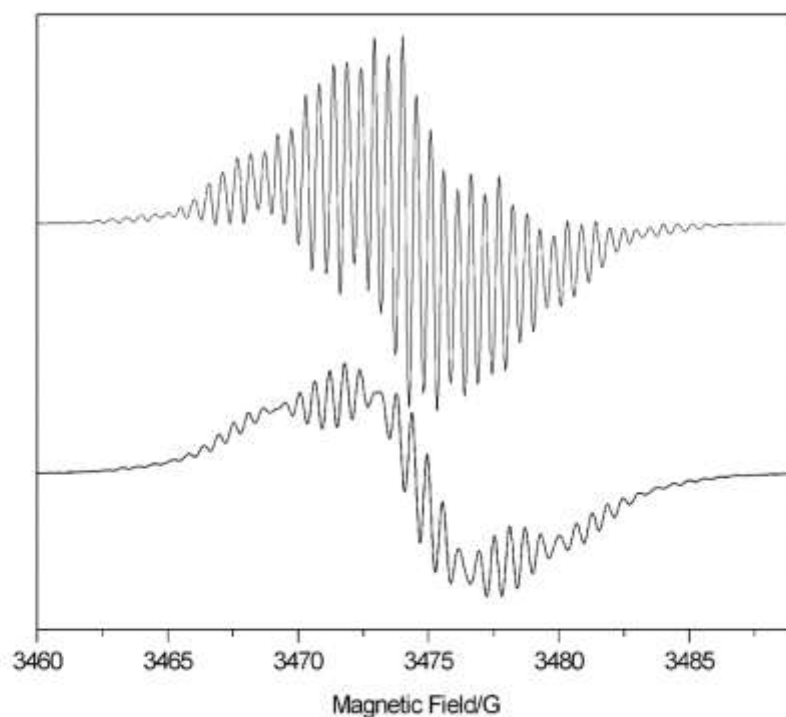


**Figure S1.** Experimental EPR spectra for electrochemically generated  $[1]^\bullet-$  (upper trace,  $g_{\text{iso}} 2.0044$ ) and  $[2]^\bullet-$  (lower trace,  $g_{\text{iso}} 2.0043$ ) in  $\text{CH}_2\text{Cl}_2$  containing  $[\text{Bu}_4\text{N}][\text{BF}_4]$  (0.4 M) at ambient temperature.

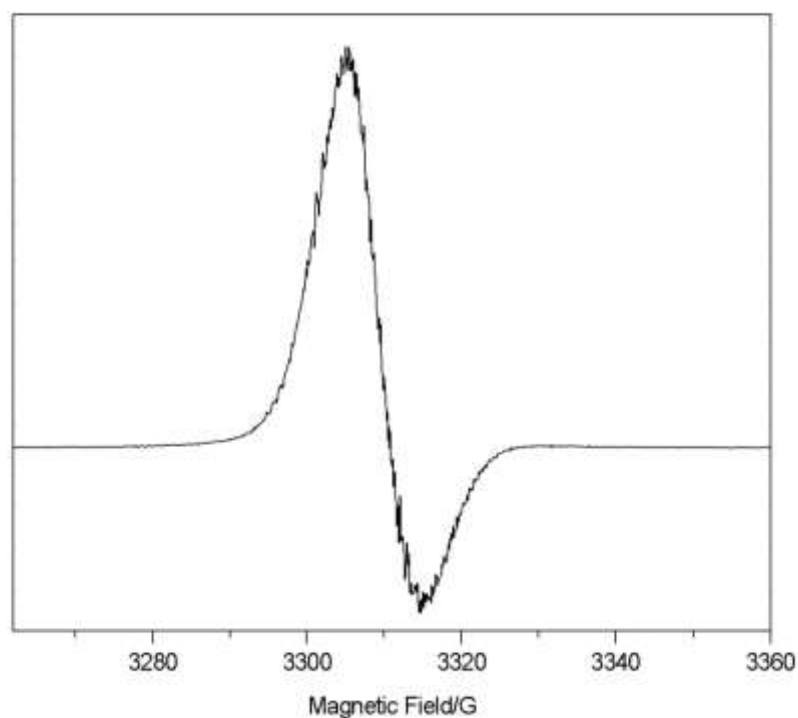


**Figure S2.** Experimental EPR spectrum for electrochemically generated  $[2]^{\bullet-}$  in  $\text{CH}_2\text{Cl}_2$  containing  $[\text{Bu}_4\text{N}][\text{BF}_4]$  (0.4 M) as a frozen glass at 77 K.

### Spectroelectrochemistry Measurements.

**Table S2.** UV-visible data obtain from spectroelectrochemistry measurements.

Compound	$\lambda_{\text{max}}/\text{nm}$ ( $\epsilon \times 10^{-4}/\text{mol dm}^{-3} \text{cm}^{-1}$ )
$[1]^0$	263 (3.0), 284 (2.9), 325 (3.6), 443 (1.0), 578 (1.2), 629 (2.0)
$[1]^{1-}$	257 (4.3), 325 (2.8), 504 (0.9), 771 (2.8), 855 (1.7)
$[1]^{2-}$	259 (4.1), 287 (3.8), 325 (2.4), 364 (2.0), 447 (0.4), 610 (3.0), 640 (3.1)
$[1]^{1+b}$	286 (2.8), 318 (3.7), 468 (1.4), 577 (1.3), 613 (1.4)
$[2]^0$	265 (7.9), 284 (8.0), 326 (8.5), 446 (2.3), 582 (3.2), 628 (4.6)
$[2]^{1-}$	262 (10.4), 325 (6.9), 507 (2.0), 769 (7.3), 853 (4.1)
$[2]^{2-}$	262 (10.0), 286 (10.2), 325 (5.9), 361 (4.8), 442 (0.9), 605 (7.7), 632 (7.9), 665 (4.4)

<sup>a</sup> obtained at a optically transparent electrode cell, in  $\text{CH}_2\text{Cl}_2$  containing  $[\text{Bu}_4\text{N}][\text{BF}_4]$  (0.4 M) at 273 K, spectral range: 230 – 900 nm. <sup>b</sup> at 243 K.

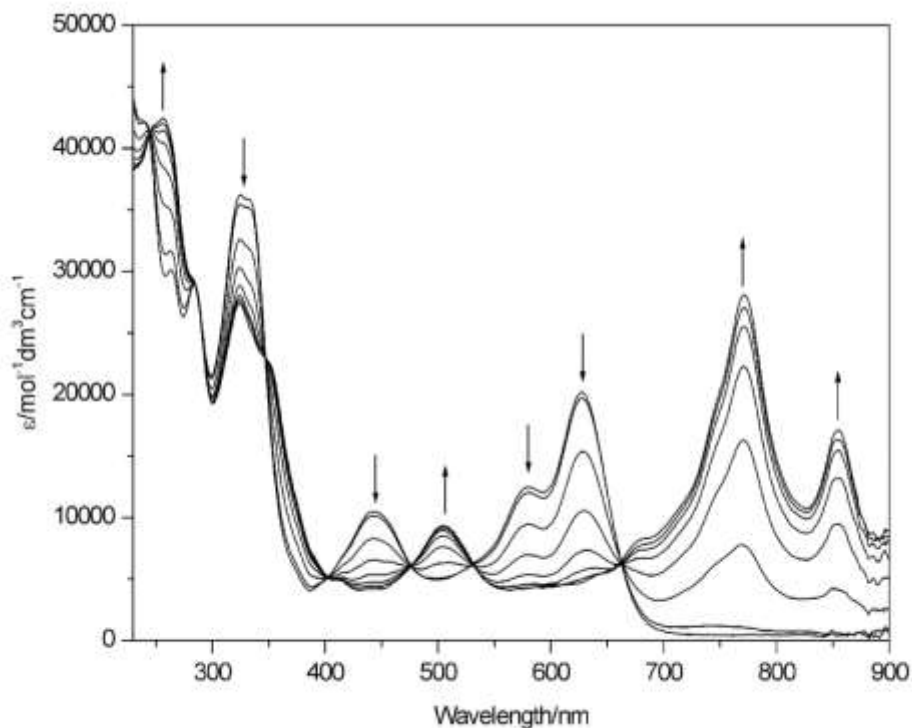


**Figure S3.** View of UV-visible spectra recorded in  $\text{CH}_2\text{Cl}_2$  containing  $[\text{Bu}_4\text{N}][\text{BF}_4]$  (0.4 M) using spectroelectrochemical methods for **1** at 273 K showing the inter-conversion of **1** to  $[\mathbf{1}]^{\bullet-}$ . Arrows indicate the progress of the reduction.

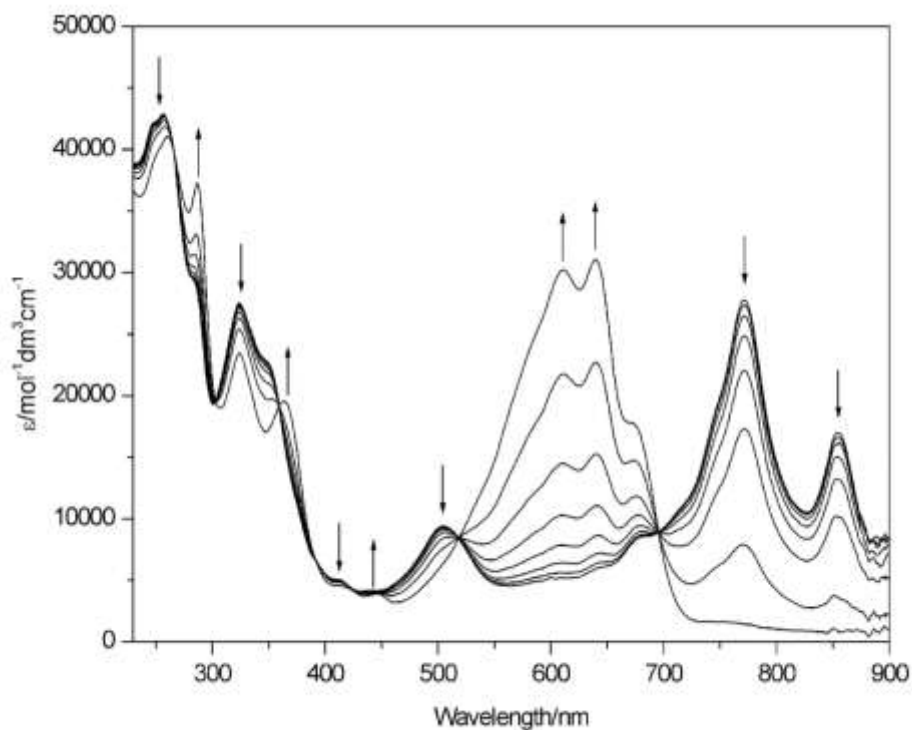


**Figure S4.** View of UV-visible spectra recorded in  $\text{CH}_2\text{Cl}_2$  containing  $[\text{Bu}_4\text{N}][\text{BF}_4]$  (0.4 M) using spectroelectrochemical methods for **1** at 273 K showing the inter-conversion of  $[\mathbf{1}]^{\bullet-}$  to  $[\mathbf{1}]^{\bullet 2-}$ . Arrows indicate the progress of the reduction.

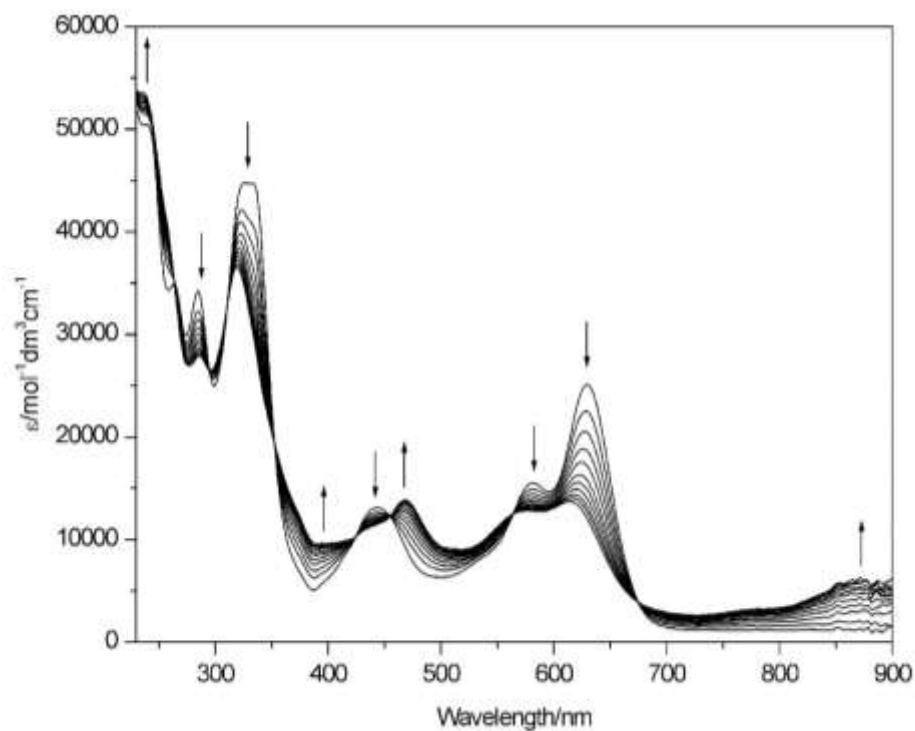
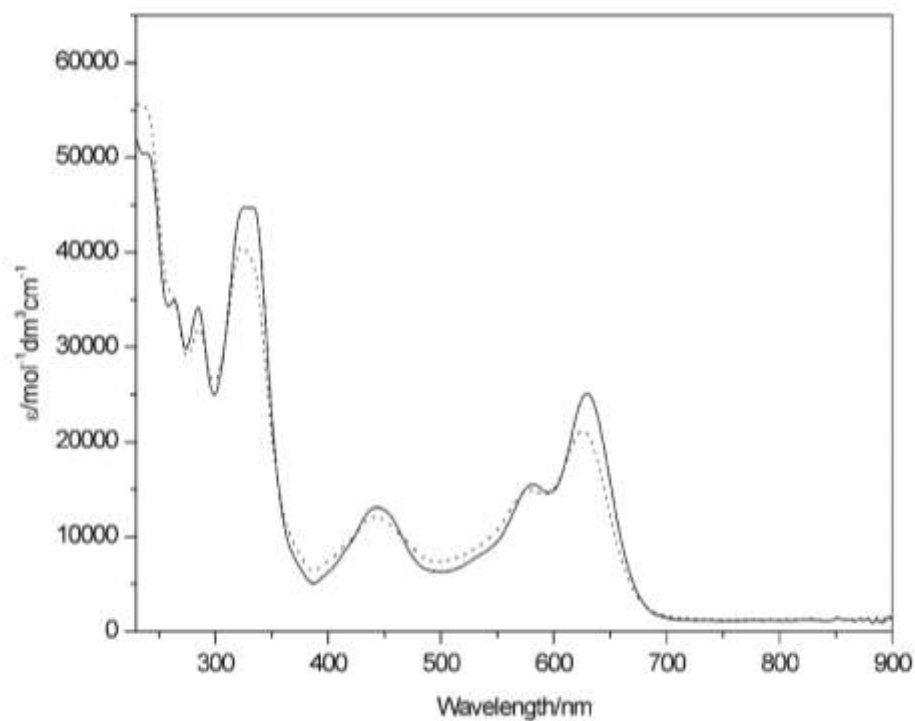


**Figure S5.** View of UV-visible spectra recorded in  $\text{CH}_2\text{Cl}_2$  containing  $[\text{Bu}_4\text{N}][\text{BF}_4]$  (0.4 M) using spectroelectrochemical methods for **1** at 243 K showing the inter-conversion of  $[\mathbf{1}]^-$  to  $[\mathbf{1}]^+$ . Arrows indicate the progress of the oxidation.



UV-visible spectra recorded in  $\text{CH}_2\text{Cl}_2$  containing  $[\text{Bu}_4\text{N}][\text{BF}_4]$  (0.5 M) for **1** at 243 K before (solid line) and after (dotted line) oxidation to  $[\mathbf{1}]^{1+}$ .

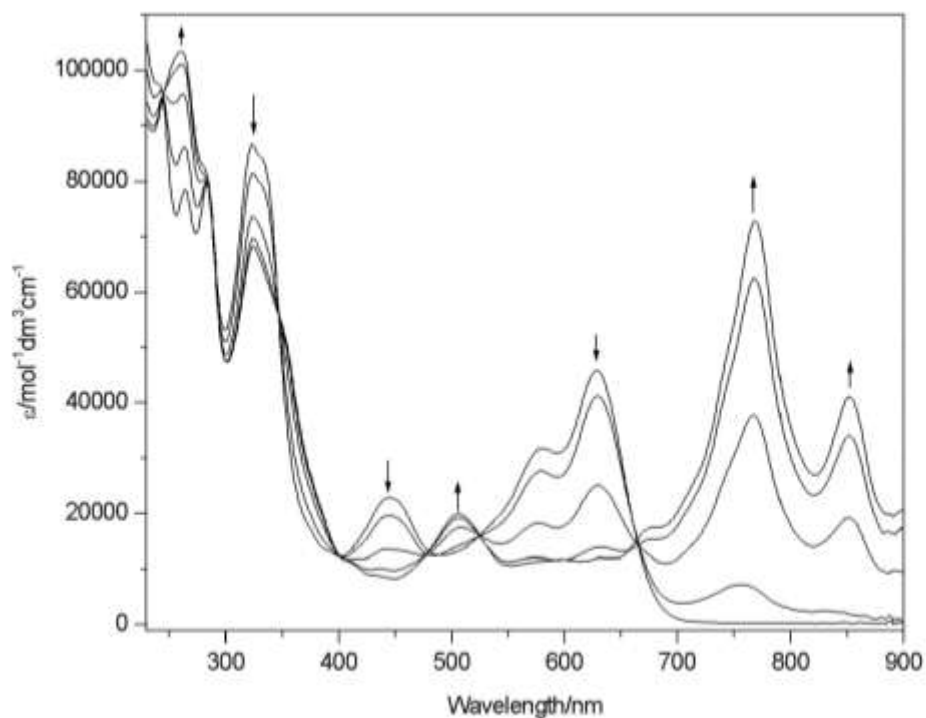


**Figure S3.** View of UV-visible spectra recorded in  $\text{CH}_2\text{Cl}_2$  containing  $[\text{Bu}_4\text{N}][\text{BF}_4]$  (0.4 M) using spectroelectrochemical methods for **2** at 273 K showing the inter-conversion of **2** to  $[\mathbf{2}]^{\bullet-}$ . Arrows indicate the progress of the reduction.

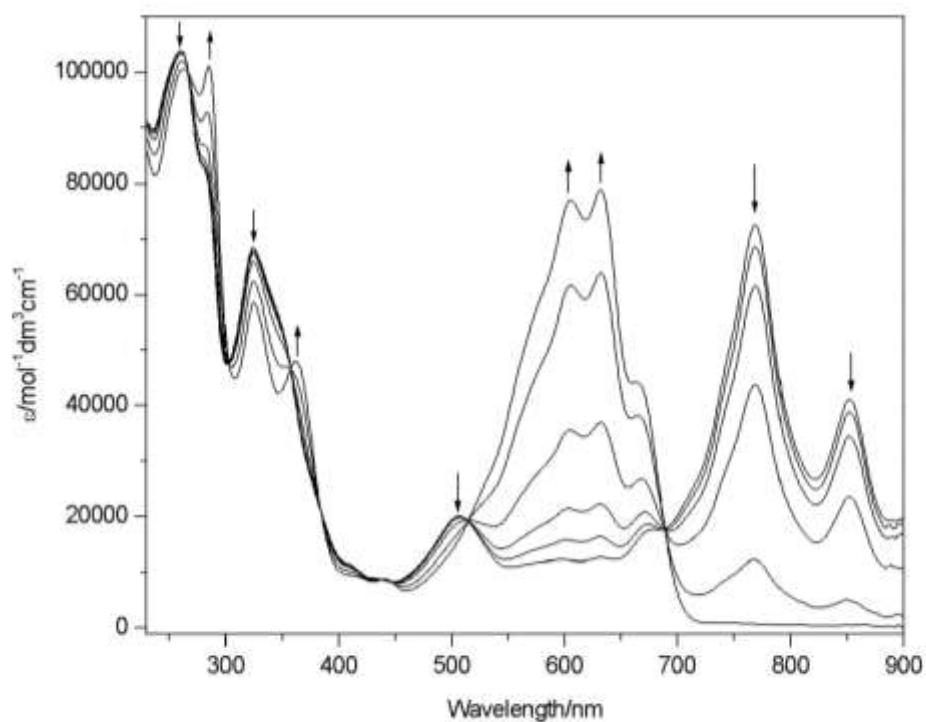


**Figure S4.** View of UV-visible spectra recorded in  $\text{CH}_2\text{Cl}_2$  containing  $[\text{Bu}_4\text{N}][\text{BF}_4]$  (0.4 M) using spectroelectrochemical methods for **2** at 273 K showing the inter-conversion of  $[\mathbf{2}]^{\bullet-}$  to  $[\mathbf{2}]^{2-}$ . Arrows indicate the progress of the reduction.

Compound	$\lambda_{\text{abs}} / \text{nm}$ ( $\epsilon / \times 10^3 \text{ M}^{-1} \text{ cm}^{-1}$ )	$\lambda_{\text{em}} / \text{nm}$ (r.t.)	$\Phi_{\text{em}}$	$\tau_{\text{em}} / \text{ns}$	$\lambda_{\text{em}} / \text{nm}$ (77 K)	$\tau_{\text{em}} / \mu\text{s}$ (77 K)
<b>2</b>	580 (31.5)	696	0.02	17	650	3.2
	629 (45.7)				700	
<b>3</b>	527 (19.9)	599	0.70	6.9	-	-
	568 (28.8)	645 (sh)			-	-

**Table 1** Photophysical properties of **2** and **3** at room temperature in dichloromethane and at 77 K in a propionitrile:butyronitrile (4:1) glass.

#### Synthesis of N,N'-Di-(*n*-butyl)-1,7-di(phenylethynyl)perylene-3,4:9,10-tetracarboxylic diimide **3**

N,N'-di-(*n*-butyl)-1,7-dibromoperylene-3,4:9,10-tetracarboxylic bisimide (1.98 g, 3 mmol) was dissolved in a mixture of dry THF (100 mL) and dry triethylamine (50 mL) under an argon atmosphere. PdCl<sub>2</sub>(PPh<sub>3</sub>)<sub>2</sub> (84 mg, 0.12 mmol), CuI (29 mg, 0.15 mmol) and phenylacetylene (1.3 mL, 12 mmol) were added and the reaction mixture was stirred at 80°C for 4 h, before being cooled to room temperature and poured into HCl (0.1 M, 100 mL). The product was extracted with dichloromethane and the organic layer washed with water until neutral, dried with Na<sub>2</sub>SO<sub>4</sub> and evaporated under reduced pressure. The resulting crude product was purified by column chromatography (SiO<sub>2</sub>, CHCl<sub>3</sub>) to give 1.77 g (84%) of a red powder. MS (MALDI-TOF): *m/z* 702.5 (M). <sup>1</sup>H NMR (CDCl<sub>3</sub>):  $\delta$  = 10.09 (d, *J* = 8.3 Hz, 2H), 8.86 (s, 2H), 8.72 (d, *J* = 8.2 Hz, 2H), 7.74-7.60 (m, 4H), 7.56-7.60 (m, 4H), 7.56-7.45 (m, 6H), 4.27 (t, *J* = 7.5 Hz, 4H), 1.80 (quin, *J* = 7.5 Hz, 4H), 1.55-1.42 (m, 4H), 1.05 (t, *J* = 7.4 Hz, 6H). <sup>13</sup>C NMR (CDCl<sub>3</sub>):  $\delta$  = 163.32, 162.99, 137.52, 134.22, 134.01, 131.90, 130.48, 129.73, 128.88, 127.68, 127.58, 127.50, 123.07, 122.18, 122.16, 120.20, 98.54, 90.73, 40.47, 30.21, 20.38, 13.87.

#### Ranges of Pt-P and Pt-C bond lengths in platinum-diacetylide diphosphine complexes.

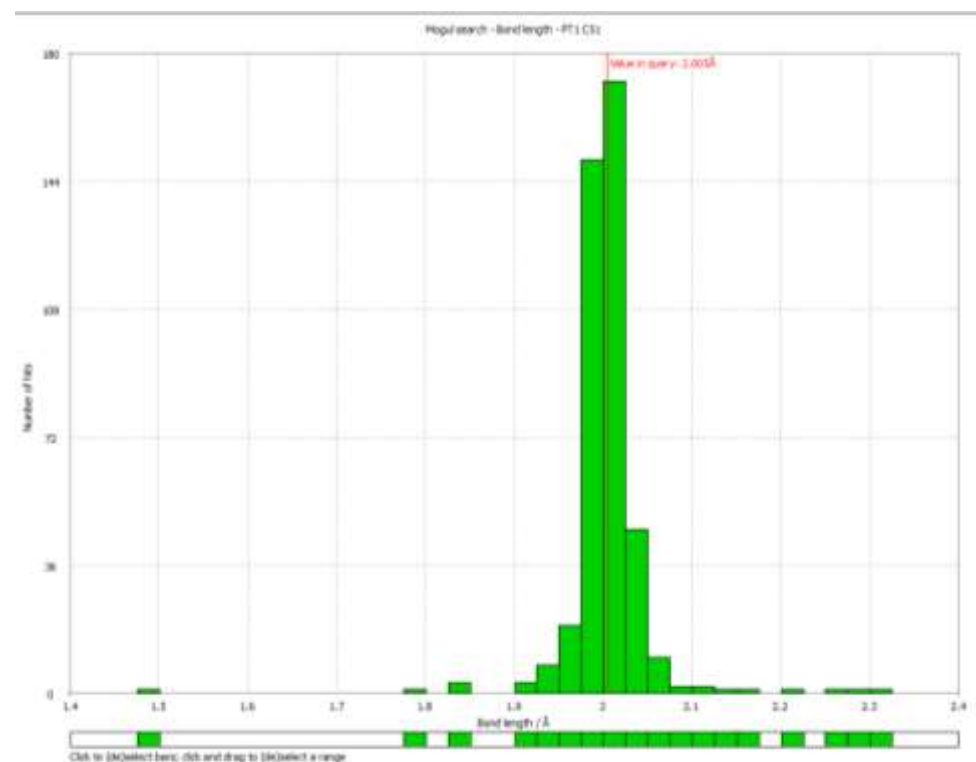


**Figure S5.** Pt-C bond lengths observed in platinum-diacetylide diphosphine complexes. The corresponding bond length observed in **1** is highlighted by a red line.

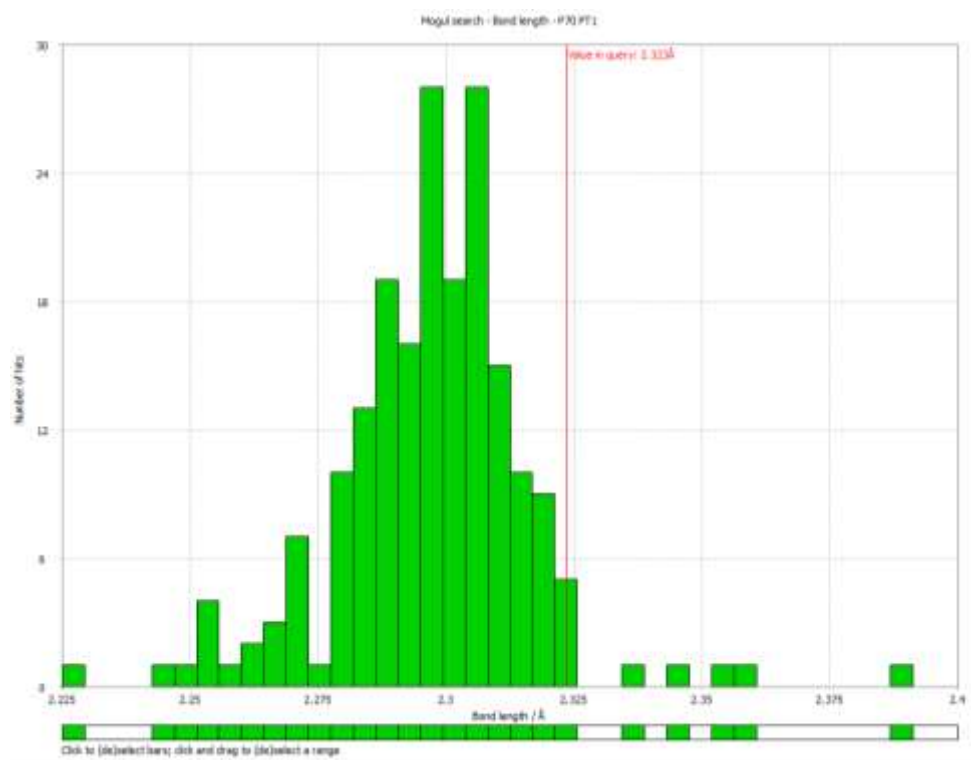


**Figure S6.** Pt-P bond lengths observed in platinum-diacetylide diphosphine complexes. The corresponding bond length observed in **1** is highlighted by a red line.